

Vibration Suppression of a Helicopter Fuselage by Pendulum Absorbers : Rigid-Body Blades with Aerodynamic Excitation Force*

Imao NAGASAKA**, Yukio ISHIDA**, Takayuki KOYAMA*** and
Naoki FUJIMATSU***

** Chubu University

1200, Matsumoto-cho, Kasugai, Aichi, 487-8501, Japan

E-mail: nagasaka@isc.chubu.ac.jp

*** Nagoya University

Furo-cho, Chikusa, Nagoya, Aichi, 464-8603, Japan

Abstract

Currently, some kinds of helicopters use pendulum absorbers in order to reduce vibrations. Present pendulum absorbers are designed based on the antiresonance concept used in the linear theory. However, since the vibration amplitudes of the pendulum are not small, it is considered that the nonlinearity has influence on the vibration characteristics. Therefore, the best suppression cannot be attained by using the linear theory. In a helicopter, periodic forces act on the blades due to the influences of the air thrust. These periodic forces act on the blades with the frequency which is the integer multiple of the rotational speed of the rotor. Our previous study proposed a 2-degree-of-freedom (2DOF) model composed of a rotor blade and a pendulum absorber. The blade was considered as a rigid body and it was excited by giving a sinusoidal deflection at its end. The present paper proposes a 3DOF model that is more similar to the real helicopter, since the freedom of the fuselage is added and the periodic forces are applied to the blade by aerodynamic force. The vibration is analyzed considering the nonlinear characteristics. The resonance curves of rotor blades with pendulum absorbers are obtained analytically and experimentally. It is clarified that the most efficient condition is obtained when the natural frequency of the pendulum is a little bit different from the frequency of the external force. Various unique nonlinear characteristics, such as bifurcations, are also shown.

Key words : Vibration Suppression, Absorber, Pendulum, Helicopter, Nonlinear Vibration,

1. Introduction

Pendulum absorbers are widely used to suppress vibrations of helicopter blades^{(1),(2)}. This utilizes antiresonance point of the vibration theory. Several works⁽³⁾⁻⁽⁷⁾ analysed the pendulum absorber based on the linear theory. However, since the pendulum oscillates with large amplitude when the resonance of the blade is suppressed, it is necessary to clarify its characteristics based on the nonlinear theory.

In the previous paper⁽⁸⁾, the authors derived a 2DOF nonlinear model for a rotor-blade-pendulum system with a base excitation, that is, the vertical deflection of the rotor was changed sinusoidally. The effect of the pendulum absorber to the blade vibration was clarified by numerical simulations and nonlinear theoretical analyses. Moreover, these results were verified by experiments.

In the present paper, in order to model a real helicopter more precisely, the freedom

*Received 23 July, 2008 (No. T2-07-0979)
Japanese Original: Trans. Jpn. Soc.
Mech. Eng., Vol.74, No.741, C (2008),
pp.1231-1237 (Received 22 Oct., 2007)
[DOI: 10.1299/jsdd.2.1230]

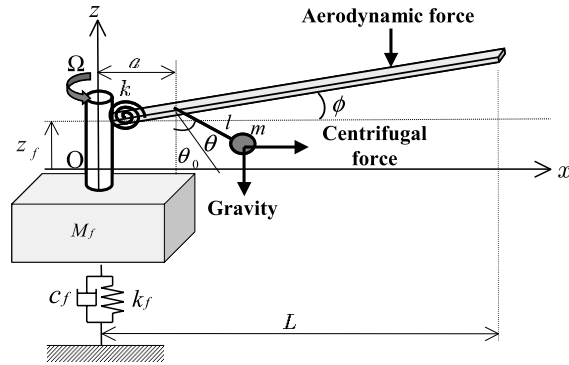


Fig. 1 Model for a fuselage, a rotor blade and a pendulum absorber

of a fuselage is considered and the periodic excitation force is given by the aerodynamic force. This 3DOF model has freedoms for a fuselage, a blade and a pendulum. The effects of pendulum parameters to the vibration suppression are investigated by numerical simulations and theoretical analyses. These results were verified by experiments.

2. Modeling and the Equations of Motion

Figure 1 shows a pendulum vibration absorber. This absorber is installed to suppress vibrations of a fuselage, a main rotor and a blade. For simplicity, the blade is assumed as a rigid beam and only its vertical displacement is considered. The helicopter is modeled as a 3DOF system where the fuselage, the blade and the pendulum have freedoms. In order to resemble the fuselage floating in the air, the mass M_f is suspended vertically by a spring with the very weak stiffness k_f . The vertical deflection is denoted by z_f . It is assumed that the fuselage does not rotate. The blade is a thin beam with a rectangular cross section. Its one end is connected to the rotor by a pin and a spring and the other end is free. Let the length of the blade be L , the mass be M and the small angle from the horizontal direction be ϕ . A pendulum with arm length l and mass m is installed at the position a from the center of the rotor. The pendulum can rotate in a vertical plane including the rotating shaft and its deflection from the equilibrium position is expressed by θ .

The diameter of the rotor is small enough to be neglected. The static rectangular coordinate system $O-xyz$ is prepared. Its x -axis is taken in the horizontal direction which coincides with the blade at rest and its z -axis is taken in the vertical direction which coincides with the rotor. The rotor and the blade rotate with the angular velocity Ω .

It is assumed that a periodic aerodynamic force works to the blade due to the periodic change of the pitch angle of the blade.

The kinetic energies T_f , T_b and T_p and the potential energies U_f , U_b and U_p of the fuselage, the blade, and the pendulum, respectively, are given as follows.

$$\left. \begin{aligned} T_f &= \frac{1}{2} M_f \dot{z}_f^2 \\ T_b &= \frac{1}{6} M \{ L^2 (\Omega^2 - \Omega^2 \phi^2 + \dot{\phi}^2) + 3 \dot{z}_f^2 + 3 L \dot{z}_f \dot{\phi} \} \\ T_p &= \frac{1}{2} m \{ \dot{z}_f^2 + a^2 \dot{\phi}^2 + l^2 \dot{\theta}^2 + \Omega^2 (a + l \sin \theta)^2 + 2 a \dot{z}_f \dot{\phi} + 2 a l \dot{\phi} \dot{\theta} \sin \theta + 2 l \dot{z}_f \dot{\theta} \sin \theta \} \end{aligned} \right\} \quad (1)$$

$$\left. \begin{aligned} U_f &= \frac{1}{2} k_f z_f^2 + M_f g z_f \\ U_b &= \frac{1}{2} k \phi^2 + \frac{1}{2} M g L (2 z_f + L \phi) \\ U_p &= m g (z_f + a \phi - l \cos \theta) \end{aligned} \right\} \quad (2)$$

where g is the acceleration of gravity. The dissipation function of the whole system is given as

$$D = \frac{1}{2}c_f \dot{z}_f^2 + \frac{1}{2}c_b \dot{\phi}^2 + \frac{1}{2}c_p \dot{\theta}^2 \quad (3)$$

where c_f , c_b and c_p are the damping coefficients of the fuselage, the blade and the pendulum, respectively.

It is assumed that the aerodynamic force distributing along the blade works periodically. The aerodynamic force is proportional to the square of the velocity. Let the magnitude of the aerodynamic load per unit length at the edge of the blade be $\Omega^2 F_b$ and its frequency be ω , the vertical force Q_b working to the fuselage, and the moment M_b around the hinge of the blade are expressed as follows.

$$\left. \begin{aligned} Q_b &= \frac{1}{3}L\Omega^2 F_b \cos \omega t \\ M_b &= \frac{1}{4}L^2\Omega^2 F_b \cos \omega t \end{aligned} \right\} \quad (4)$$

Putting $P_0 = \sqrt{3k/ML^2}$ and introducing h_0 as a representative length, we use the following dimensionless quantities.

$$\left. \begin{aligned} \bar{z}_f &= z_f/h_0, & \bar{m} &= m/M, & \bar{M}_f &= M_f/M \\ \bar{c}_f &= c_f/MP_0, & \bar{c}_b &= c_b/Mh_0^2P_0, & \bar{c}_p &= c_p/Mh_0^2P_0 \\ \bar{L} &= L/h_0, & \bar{l} &= l/h_0, & \bar{a} &= a/h_0 \\ \bar{k}_f &= k_f/MP_0^2, & \bar{F}_b &= F_b/M, & \bar{g} &= g/(h_0P_0^2) \\ \bar{\Omega} &= \Omega/P_0, & \bar{\omega} &= \omega/P_0, & \bar{t} &= p_0t \end{aligned} \right\} \quad (5)$$

Using Lagrange's equation, we obtain the following nonlinear equations expressed by dimensionless quantities. For simplicity, the notation “-” which represents a dimensionless quantity is eliminated in the following.

$$\left. \begin{aligned} (1 + m + M_f)\ddot{z}_f + \left(\frac{1}{2}L + ma\right)\ddot{\phi} + ml(\ddot{\theta} \sin \theta + \dot{\theta}^2 \cos \theta) \\ + c_f \dot{z}_f + k_f z_f &= \frac{1}{3}L\Omega^2 F_b \cos \omega t - (1 + m + M_f)g \\ \left(\frac{1}{2}L + ma\right)\ddot{z}_f + \left(\frac{1}{3}L^2 + ma^2\right)\ddot{\phi} + mal(\ddot{\theta} \sin \theta + \dot{\theta}^2 \cos \theta) \\ + c_b \dot{\phi} + \frac{1}{3}L^2(1 + \Omega^2)\phi &= \frac{1}{4}L^2\Omega^2 F_b \cos \omega t - \left(\frac{1}{2}L + ma\right)g \\ \ddot{z}_f \sin \theta + a\ddot{\phi} \sin \theta + l\ddot{\theta} + \frac{c_p}{ml}\dot{\theta} - \Omega^2(a + l \sin \theta) \cos \theta + g \sin \theta &= 0 \end{aligned} \right\} \quad (6)$$

3. Tuning of a Pendulum

In a high rotational speed range, the centrifugal force becomes much larger than the gravitational force. In such a case, the natural frequency of the pendulum is expressed as $p_p \approx \Omega \sqrt{1 + a/l}$ approximately. Therefore, it is proportional to the rotational speed Ω . Since the excitation frequency ω is n times the rotational speed Ω , the natural frequency of the pendulum always tunes to the excitation frequency ω if we determine the pendulum to satisfy the relationship $n = \sqrt{1 + a/l}$.

The present paper shows the case of $n = 4$. Results of numerical simulation are shown in Fig. 2. This shows the natural frequencies p_f , p_b and p_p of the fuselage, the blade and the pendulum are the function of the rotational speed Ω . These p_f , p_b and p_p are obtained from the equation which is derived from Eq. (6) by eliminating the coupling terms and damping terms. This indicates that the natural frequency p_p of the pendulum satisfies the tuning condition $\omega = 4\Omega$ except in the low rotational speed range $\Omega < 0.15$. Therefore, the vibration suppression effect in the wide range of the rotational speed Ω can be possible.

4. Results of Numerical Simulation

The following results are obtained by integrating Eq. (6) numerically.

4.1. Case of the Tuned Pendulum

Figure 3 shows the effects of the pendulum to the amplitudes of the fuselage and the blade. The cases with a pendulum and those without a pendulum are compared. The vibration of the blade and the fuselage are well suppressed by the installation of the pendulum absorber. Since the most effective results are obtained in the case that the value $\sqrt{1+a/l}$ is shifted a little from the value of 4 as explained later in Fig. 8⁽⁸⁾, the result for $\sqrt{1+a/l} = 3.90$ is shown. The following values are used for the other parameters: $M_f = 50.0$, $m = 0.2$, $L = 600.0$, $a = 200.0$, $k_f = 0.1$, $c_f = 0.05$, $c_b = 15000$, $c_p = 5.0$, $F_b = 0.05$, $h_0 = 0.001[\text{m}]$, $P_0 = 10.0 \times 2\pi$.

The amplitudes of the fuselage and the blade increased a little due to the pendulum installation in the higher rotational speed range. As explained later, this occurs because this method utilizes the antiresonance point and the most appropriate dimensions of the pendulum differs a little depending on the rotational speed.

4.2. Influence of the Excitation Force

Figure 4 shows the influence of the magnitude of the excitation force on the maximum amplitude of the fuselage vibration in the tuned condition.

The effect of the pendulum decreases as the excitation force increases and the effect disappears above $F_b = 0.17$ due to the rotation of the pendulum. This shows that the pendulum has a limit of its effect due to the nonlinearity of the pendulum restoring force.

4.3. Influence of the Position of the Pendulum

The effect of pendulum at the position $(2/3)L$ from the rotor is shown in Fig. 5.

From the comparison between Figs. 3 and Fig. 5, it becomes clear that the effect increases as the pendulum is attached at far away place from the rotor. The limit of the magnitude of the excitation force which

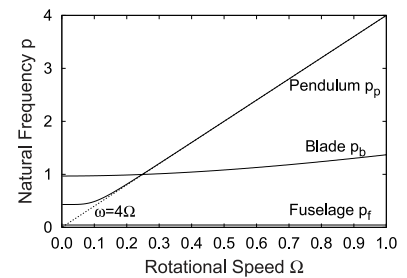
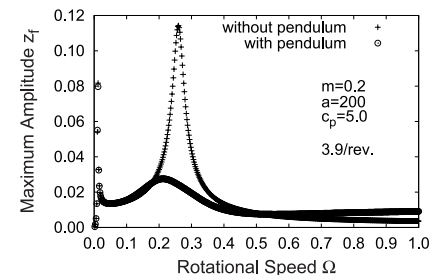
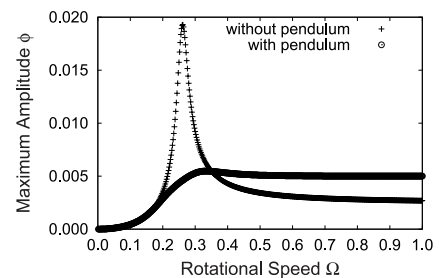


Fig. 2 Natural frequencies of the blade and the pendulum (case of tuned enough)



(a) fuselage



(b) blade

Fig. 3 Resonance curves

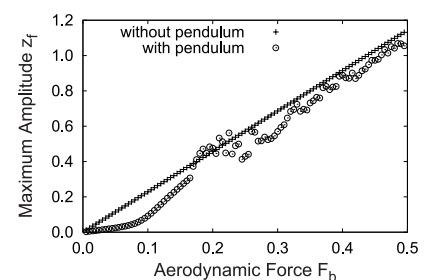


Fig. 4 Influence of the amplitude of harmonic excitation

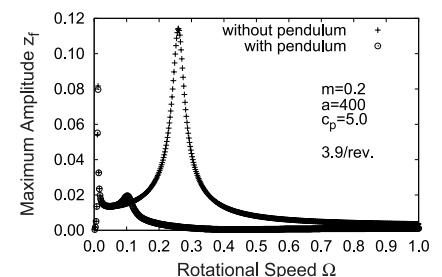


Fig. 5 Influence of the mounted position a

works effectively increases as the position becomes far from the rotor. These changes are due to the increase of the centrifugal force depending on the position of the pendulum.

4.4. Influence of the Pendulum Mass Ratio

The influence of the mass ratio of the blade and pendulum are shown in Fig. 6.

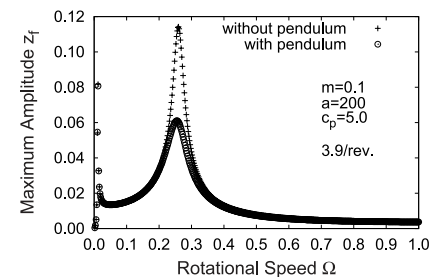
From the comparison of Figs. 3 and 6, it is known that a larger mass is more effective. However, undesirable effect in the high speed range increase.

4.5. Influence of the Damping

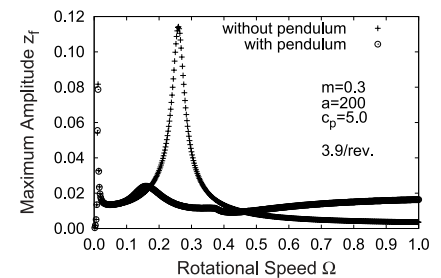
Figure 7 shows the influence of the pendulum damping c_p . This is the case that the damping coefficient is two times that of the case of Fig. 3 where $c_p = 5.0$. As the damping coefficient increases, the minimum amplitude at the antiresonance point increases. As the result, since this pendulum absorber utilizes this antiresonance, the effect decreases. However, as will be explained in Fig. 10 later, a pendulum start rotating at a smaller excitation force when the damping decreases.

4.6. Influence of the Tuning

As mentioned above, the natural frequency of the pendulum is given by $p_p \approx \Omega \sqrt{1 + a/l}$ which is proportional to the rotational speed Ω . Therefore, its coefficient must be tuned to the excitation frequency. When the position of the pendulum, a , is constant, the natural frequency of the pendulum is determined solely by the pendulum arm length l . Namely, tuning is executed by adjusting the length. Figure 8 shows the effect of the tuning when the rotational speed is $\Omega = 0.26$ which is the major critical speed. This figure indicates us that the most effective pendulum natural frequency is not 4Ω but 3.90Ω . The reason why the most appropriate tuning shifts from 4 is the same as that explained in the previous paper⁽⁸⁾. Since the rated rotational speed is different from each other in helicopters, the most appropriate dimensions of the pendulum must be determined by using such a diagram as Fig. 8.



(a) $m = 0.1$



(b) $m = 0.3$

Fig. 6 Influence of the pendulum mass m

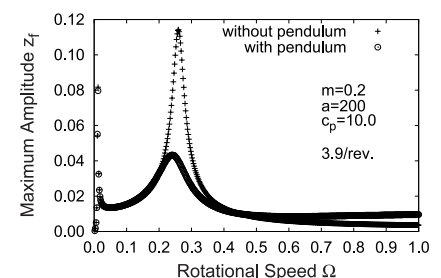


Fig. 7 Influence of the damping coefficient c_p

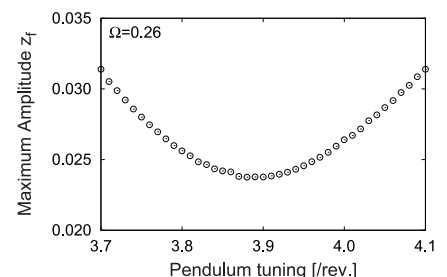


Fig. 8 Influence of the pendulum tuning

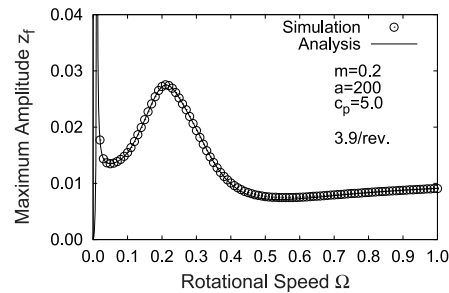


Fig. 9 Analytical result

5. Theoretical Analysis

5.1. The Method of van der Pol

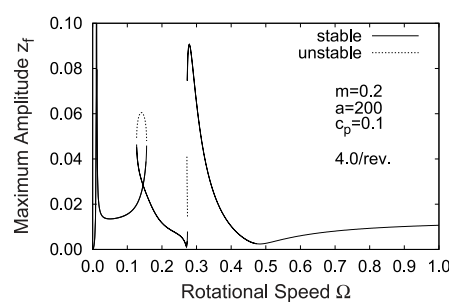
We analyse by the method of van der Pol. First, the term $\sin \theta$ and $\cos \theta$ in Eq. (6) is replaced by the power series approximation up to the third order of θ . We assume the solution as follows.

$$\left. \begin{aligned} z_f &= Z_s \sin \omega t + Z_c \cos \omega t \\ \phi &= \Phi_s \sin \omega t + \Phi_c \cos \omega t \\ \theta &= \Theta_s \sin \omega t + \Theta_c \cos \omega t \end{aligned} \right\} \quad (7)$$

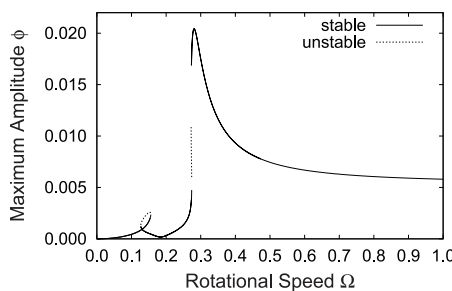
where it is assumed that $Z_s, Z_c, \Phi_s, \Phi_c, \Theta_s$ and Θ_c have magnitudes of $O(\epsilon^0)$ when ϵ represents a small parameter and O means the order. In addition, it is assumed that these quantities change slowly as a function of time.

Substituting Eq. (7) into Eq. (6) and equating the coefficients of terms $\cos \omega t$ and $\sin \omega t$ in both hands in the accuracy of $O(\epsilon)$, respectively, we obtain the first order differential equations on $Z_s, Z_c, \Phi_s, \Phi_c, \Theta_s$ and Θ_c . The steady-state solutions are obtained from the equations which are obtained by putting $\dot{Z}_s = 0, \dot{Z}_c = 0, \dot{\Phi}_s = 0, \dot{\Phi}_c = 0, \dot{\Theta}_s = 0$ and $\dot{\Theta}_c = 0$. The stability of these solutions are determined by investigating the change of a small deviation around the steady-state solution.

The results of the theoretical analysis are shown in Fig. 9 together with the results of numerical simulation. The full lines shows the results of theoretical analyses and the symbol

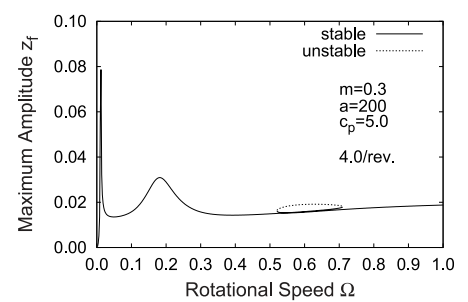


(a) fuselage

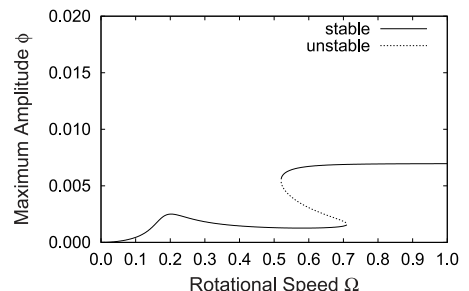


(b) blade

Fig. 10 Nonlinear branches ($c_p = 0.1$)



(a) fuselage



(b) blade

Fig. 11 Nonlinear branches ($m = 0.3$)

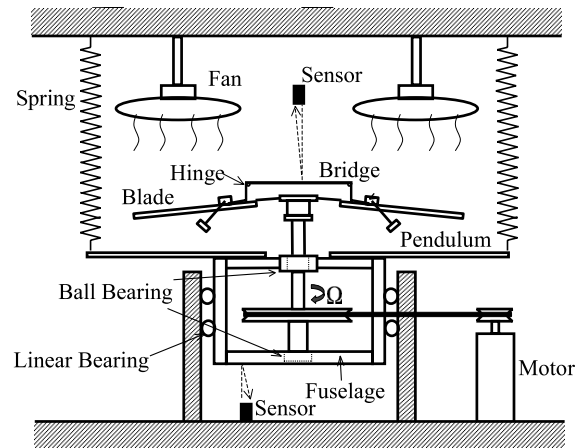


Fig. 12 Model of experimental set-up

○ shows the results of numerical solution. Both results agree well.

5.2. Nonlinear Bifurcation Phenomena

Here, the bifurcation phenomena due to the nonlinearity is discussed. One parameter is changed from the case of Fig. 9. The case that the damping coefficients $c_p = 0.1$ is shown in Fig. 10 and the case of the mass ratio $m = 0.3$ is shown in Fig. 11. The full lines represent stable solutions and the broken lines represent unstable solutions. The theoretical curve forms a loop in the neighborhood of $\Omega = 0.15$ in Fig. 10 and that of $\Omega = 0.6$ in Fig. 11 and unstable solutions exist there. This is because that the effect of the nonlinearity becomes apparent when the amplitude of the pendulum increases. As the shape and the stability of the resonance curve change remarkably depending on the parameter values, there is a danger that large vibrations may appear.

6. Experiments

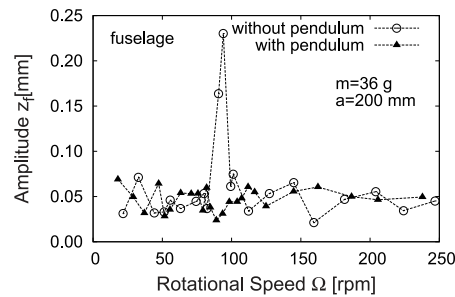
6.1. Experimental Setup

Figure 12 shows the experimental setup of the study. The fuselage with mass $M_f = 5.38$ kg is hung by a weak spring with the spring constant $k_f = 0.047$ N/mm from the ceiling. It is guided to move only in a vertical direction by linear guides. The rotor is supported by self-aligning ball bearings at the upper and lower parts of the fuselage. The shaft is driven by a motor via pulleys and a belt. A flange is attached at the upper end of the shaft and two thin plate springs with the spring constant $k = 0.0413$ N·m/rad are mounted on this flange symmetrically. Further, two rigid long plates which correspond to blades are attached to these springs. This plate is made of aluminum with the mass density $\rho = 2698$ kg/m³ and has the mass $M = 60$ g. Its dimensions are $L = 300$ mm in length, $b = 50$ mm in width and $h_b = 1.5$ mm in thickness. Pendulums can be mounted at the position $a = 200$ mm, 260 mm and 330 mm on the blade. The arm lengths of the pendulums can be changed. The three kinds of masses with $m = 12$ g, 24 g and 36 g are used. In order to measure the vertical displacement of the blades in the case that two blades vibrate in the same direction, a bridge which is a very light plate is connected to the blades via hinges. A periodic aerodynamic force with the frequency 4 times the rotational speed is applied by four fans.

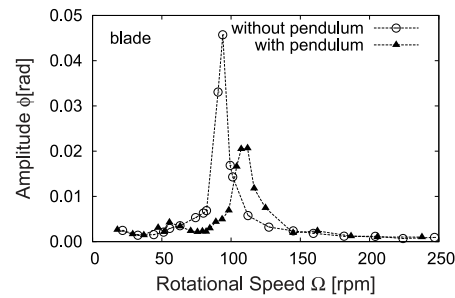
Vertical deflections of the fuselage and blades are detected by laser deflection sensors and the rotational speed is detected by a rotary encoder.

6.2. Experimental Results

Figure 13 shows resonance curves of the fuselage and the blade in cases without pendulum and with pendulums at $a = 200$ mm. The data represent amplitudes of the component 4Ω which is obtained from the time histories recorded in experiments.

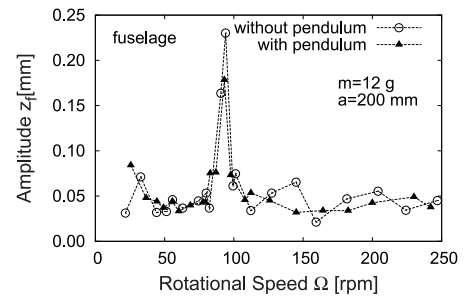


(a) fuselage

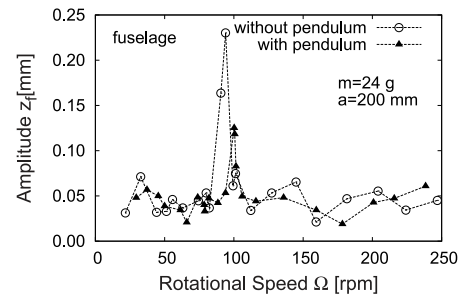


(b) blade

Fig. 13 Resonance curve (experiment)



(a) $m = 12$ g



(b) $m = 24$ g

Fig. 14 Influence of the pendulum mass m (experiment)

In the case without pendulum, the blades resonate and, as the result, the fuselage vibrates with large amplitude. In the case with pendulums, vibrations of both the fuselage and the blades are well suppressed.

Next, the effect of the pendulum mass is investigated. Figure 14 shows resonance curves for $m = 12$ g and $m = 24$ g. In the case of Fig. 14(a) with $m = 12$ g, the effect is not clear because the mass is too small to suppress vibrations. In the case of Fig. 14(b) with $m = 24$ g, the amplitude in the resonance range $\Omega = 80$ rpm to 95 rpm is well suppressed, however, it is not suppressed $\Omega = 95$ rpm to 100 rpm. These results shows that the mass is not enough in these two cases. On the contrary, Fig. 13 with $m = 36$ g shows good suppression results.

These results confirm the results of numerical simulation shown in Fig. 6.

7. Conclusions

This study investigates the vibration suppression effects of pendulum vibration absorbers to a helicopter using a 3DOF model composed with a fuselage, a blade and a pendulum. It is assumed that an aerodynamic force with frequency of 4 times the rotational speed works to the blade. The following can be made through the theoretical analysis, numerical simulations and experiments.

- i. When the natural frequency of the pendulum is tuned to the frequency of the excitation, vibrations can be suppressed by the pendulum vibration absorber in a wide rotational speed range.
- ii. As the magnitude of the excitation force increases, the effect decreases and then stops when the pendulum rotates.
- iii. As the location of the pendulum separates from the shaft, the vibration suppression effect increases.
- iv. As the mass of the pendulum increases, the vibration suppression effect increases.
- v. As the damping of the pendulum increases, the effect decreases. However, as the damping decreases, the pendulum starts to rotate at smaller excitation frequency and the effect disappears.
- vi. Better suppression effect is obtained if the pendulum frequency is tuned to a value slightly smaller than the excitation frequency.
- vii. The occurrence of bifurcation due to the pendulum is clarified.

References

- (1) Saito, K., Yamauchi, N., Yoshimura, T., Yamanaka, T., Yasuhara, H., Uemura, M. and Sato, H., Helicopter Second Edition (in Japanese), *Japan Aeronautical Engineers' Association*, (1993).
- (2) Kato, K. and Imanaga, I., Introduction to Helicopter (in Japanese), *University of Tokyo Press*, (1985), pp. 197-203.
- (3) Taylor, R.B. and Teare, P.A., Helicopter Vibration Reduction with Pendulum Absorbers, *Journal of the American Helicopter Society*, Vol.20, No.3, (1975), pp. 9-17.
- (4) Amer, K.B., and Neff, J.R., Vertical-Plane Pendulum Absorber for Minimizing Helicopter Vibratory Loads, *Journal of the American Helicopter Society*, Vol.19, No.4, (1974), pp. 44-48.
- (5) Viswanathan, S.P. and McClure, R.D., Analytical and Experimental Investigation of a Bearingless Hub-Absorber, *Journal of the American Helicopter Society*, Vol.28, No.3, (1983), pp. 47-55.
- (6) Hamouda, M.N. and Pierce, G.A., Helicopter Vibration Suppression Using Simple Pendulum Absorber on the Rotor blade, *Journal of the American Helicopter Society*, Vol.29, No.3, (1984), pp. 19-29.
- (7) Murthy, V.R. and Hammond, C.E., Vibration Analysis of Rotor blades with Pendulum Absorbers, *Journal of Aircraft*, Vol.18, No.1, (1981), pp. 23-29.
- (8) Nagasaka, I., Ishida, Y., Koyama, Y. and Fujimatsu, N., Vibration Suppression of Helicopter Blades by Pendulum Absorbers (Analytical and Experimental Investigation in Case of Rigid-Body Mode) (in Japanese), *Transactions of the Japan Society of Mechanical Engineers*, Vol.C, No.73, (2007), pp. 129-137.